J Appl Physiol 106: 1618–1630, 2009.
First published February 19, 2009; doi:10.1152/japplphysiol.91115.2008.

Mechanical efficiency of limb swing during walking and running in guinea fowl (*Numida meleagris*)

Jonas Rubenson and Richard L. Marsh

Department of Biology, Northeastern University, Boston, Massachusetts

Submitted 20 August 2008; accepted in final form 14 February 2009

Rubenson J, Marsh RL. Mechanical efficiency of limb swing during walking and running in guinea fowl (*Numida meleagris*). *J Appl Physiol* 106: 1618–1630, 2009. First published February 19, 2009; doi:10.1152/japplphysiol.91115.2008.—Understanding the mechanical determinants of the energy cost of limb swing is crucial for refining our models of locomotor energetics, as well as improving treatments for those suffering from impaired limb-swing mechanics. In this study, we use guinea fowl (*Numida meleagris*) as a model to explore whether mechanical work at the joints explains limb-swing energy use by combining inverse dynamic modeling and muscle-specific energetics from blood flow measurements. We found that the overall efficiencies of the limb swing increased markedly from walking (3%) to fast running (17%) and are well below the usually accepted maximum efficiency of muscle, except at the fastest speeds recorded. The estimated efficiency of a single muscle used during ankle flexion (tibialis cranialis) parallels that of the total limb-swing efficiency (3% walking, 15% fast running). Taken together, these findings do not support the hypothesis that joint work is the major determinant of limb-swing energy use across the animal's speed range and warn against making simple predictions of energy use based on joint mechanical work. To understand limb-swing energy use, mechanical functions other than accelerating the limb segments need to be explored, including isometric force production and muscle work arising from active and passive antagonist muscle forces.

inverse dynamics; locomotion; metabolic cost; mechanical work; guinea fowl; muscle efficiency

THAT MECHANICS AND ENERGETICS should be linked during legged locomotion seems obvious. However, establishing such links in vivo has proven elusive, even in limb swing (the swing phase of gait), during which the mechanical energy of the limb segments changes predictably; during legged locomotion (walking and running), the swing limb must accelerate from a velocity that is initially less than the body's center of mass to a velocity greater than that of the center of mass. The positive work to accomplish this task might logically be assumed to come from the muscles active during swing. However, limb swing is often compared with a pendulum, in which the motions of the leg can be generated passively via an exchange of gravitational potential and kinetic energy (40). Successful implementation of passive-dynamic robots demonstrates the feasibility of this mechanism (7). If the swing pendulum were operative in vivo, limb swing could, under appropriate conditions, be passive and require little or no metabolic energy to perform the needed mechanical work.

Of course, electromyography (EMG) studies make it clear that limb swing is not passive (22, 62), and accumulating evidence suggests limb-swing muscles use considerable metabolic energy, during both walking and running. The most direct estimates of limb-swing costs during constant-speed locomotion are based on regional blood flow measurements during treadmill locomotion in the guinea fowl *Numida meglearis*, an ~1.5-kg bird (Table 1). These studies have found that the metabolic cost of limb swing accounts for approximately one-fourth of the metabolic cost of both level walking and running and incline running (14, 35, 49). The high cost of limb swing is not unique to this bird species. Using a swing-assist mechanism, the metabolic cost of limb swing in humans has been estimated to be 20% of the total cost of running (41) and 10% of walking (23). These studies likely underestimate the total cost of limb swing slightly, given that they only reduced the work required to accelerate the limb in the first half of swing. Finally, stationary limb-swing experiments aimed to mimic walking in humans found limb-swing costs as high as 30% of total walking costs (10).

Both mechanical work and force production have been separately proposed as determinants of locomotor energy cost, including the cost of limb swing (11, 27, 37, 48). Nevertheless, a clear explanation for limb-swing energetics remains elusive, primarily because of the ambiguity of both mechanical and metabolic energy use. In the present study we use guinea fowl as a model to explore the question of whether mechanical work is a major determinant of limb-swing cost. Guinea fowl are an ideal model system, both because they are amenable to invasive experiments not possible in humans, and because their gait mechanics exhibit remarkable similarities between human locomotion, including whole body and joint mechanics (8, 16). This model system can, therefore, prove important not only for general models of limb swing, but also for studying the clinical implications of swing mechanics and energetics. Altered limb-swing mechanics occur in lower extremity amputees (9, 51) and is prevalent in several musculoskeletal disorders, in particular cerebral palsy, as a result of stiff-knee gait (3, 56). Compromised limb-swing mechanics is a potentially large contributor to the elevated metabolic cost of walking in these individuals (50, 58), and, therefore, the factors influencing limb-swing cost are important for physicians, bioengineers, and therapists aiming to improve gait performance and energy use. In particular, a positive link between limb-swing mechanical work and energetics can facilitate the prediction of limb-swing energy use in these clinical groups based on routine gait analyses.

This work tested the hypothesis that mechanical work is a major determinant of the cost of limb swing in normal walking and running. This straightforward hypothesis is suggested by the strong correlation between mechanical and metabolic energy use in limb loading in guinea fowl (14, 36) and humans (48) and the increase with speed of both the me-

Address for reprint requests and other correspondence: J. Rubenson, School of Sport Science, Exercise & Health, The Univ. of Western Australia, 35 Stirling Hwy, Crawley, WA 6009, Australia (e-mail: Jonas.Rubenson@uwa.edu.au).

Table 1. *Summary of estimated energy use in limb swing during level locomotion in guinea fowl based on the distribution of blood flow to the leg muscles*

	%Total Leg Muscle Energy Use During Swing	
Speed, m/s	50% FT	No FT
0.5*	25	21
1.5*	26	20
1.5†	27	21
1.5‡	28	23
2.4‡	29	23
2.7*	27	21
Means	27	22

The femerotibialis (FT) muscle is active in both swing and stance, and the precise distribution of energy use is not known. Separate estimates are shown assuming that 50% of the FT energy use is in swing and that none of the FT energy use is in swing. *Refs. 13, 35; †Ref. 14; ‡Ref. 49.

chanical and metabolic energy of limb swing (35, 36, 60). This hypothesis can only be evaluated in the context of the corollary hypothesis that the mechanical efficiency of limb-swing work output, both for the limb as a whole and at the muscle level, remains constant across speed. If the major function of the swing-phase muscles is the production of mechanical work, a second corollary hypothesis is suggested: that the muscles operate under conditions to maximize efficiency, and thus the limb-swing and muscle mechanical efficiencies should approximate the maximal efficiency for aerobically functioning muscle (~25%; Refs. 54, 63). One problem at the outset with the straightforward correlation between work and energy use is that the only studies directly measuring muscle energy use of swing-phase muscles in guinea fowl has found that the cost of limb swing is a constant fraction of the total locomotor cost at all speeds (13, 14, 35, 49), whereas it may be expected that limb-swing work increases curvilinearly with speed. This has been shown in the lower limb segmental work in guinea fowl (36) and of the kinetic energy of the limbs of guinea fowl relative to the center of mass (16). However, whether these approaches for calculating limb-swing work accurately reflect the mechanical work of the limb has been contested (65).

These hypotheses were tested by combining mechanical work calculated during limb swing with energy use in individual limb-swing muscles, thus providing the first estimates of the mechanical efficiency of limb swing during unmanipulated locomotion (no limb loading or unloading). We computed total limb-swing efficiencies using mechanical work measures from inverse dynamic modeling and muscle-specific energetics obtained from oxygen consumption and blood flow measurements over a range of walking and running speeds in guinea fowl. To gain further insight into the mechanics and energetics of limb swing, we also estimated, for the first time in vivo, the mechanical efficiency of an individual limb-swing muscle, the tibialis cranialis.

METHODS

Animals

Guinea fowl (*Numida meleagrisis* L.) were purchased as hatchlings from The Guinea Farm (New Vienna, IA) and were cage reared at the Northeastern University Division of Laboratory Medicine. Birds had unlimited access to food and water and were maintained on a 12:12-h light-dark cycle. At the time of the measurements, the experimental animals' ($N = 5$) body mass was 1.40 ± 0.21 kg (mean ± SD; three females, two males). All experiments were performed under protocols approved by the Northeastern University Institutional Animal Care and Use Committee.

Anatomical Modeling

Because the experimental animals used for inverse dynamic modeling were also used in other parallel studies that required dissection of the limb musculature, three separate animals were utilized for body segment measurements. These animals had a similar mass (1.64 ± 0.11 kg, mean ± SD; two females, one male) and stature compared with the experimental animals.

The major hindlimb segments of the left limb were disarticulated, weighed, and subsequently frozen. These limb segments included the thigh (femur), shank (tibiotarsus), tarsometatarsus, proximal phalanx, distal phalanges, and the body segment (Fig. 1). The masses of the segments were subsequently expressed as a fraction of the total body mass (Table 2). The center of mass of each frozen segment was determined using a suspension technique (2), and the location of the center of mass of each segment was expressed in the segment coordinate system (SCS; Fig. 1, Table 2) as a fraction of the segment length (Table 2).

The moment of inertia of each segment was measured using a pendulum method. A small hole was drilled through the proximal or distal end of the frozen segment, allowing the segment to rotate around a steel rod (3-mm diameter). The segment was perturbed, and its period of oscillation was determined by videoing the segment (500-Hz field rate; NAC-1000, NAC Image Technology, Simi Valley, CA). The moment of inertia of the segment about the axis of rotation (I_a) was calculated as:

$$I_a = \frac{m_s g L_{a,cm} t_p^2}{4\pi^2} \quad (1)$$

where I_a is in kg/m^2, m_s is segment mass (in kg), $L_{a,cm}$ is the distance from the center of mass of the segment to the axis of rotation (in m), t_p is the period of oscillation (in s), and g is the gravitational constant (9.81 m/s^2). The moment of inertia about the axis through the segments center of mass (I_{cm}) was subsequently determined using the parallel axis theorem:

$$I_{cm} = I_a - m_s L_{a,cm}^2 \quad (2)$$

where I_{cm} is in kg/m^2.

The accuracy of the segment moment of inertia depends largely on an accurate measurement of the center of mass and the period of oscillation. Locating the center of mass was limited by the resolution of our static images (minimum 100 pixels/cm) and was located accurately to ~1 mm. The period of oscillation was limited by the time between one video frame (0.002 s). The potential percent error in I_{cm} due to center of mass location was ~2% in the largest segment (femur) and ~3.5% in the smallest segment (distal phalanx). The potential percent error in I_{cm} due to the period of oscillation measurement was ~2% in all segments.

To facilitate scaling the moment of inertia to the experimental animals, we calculated the radius of gyration of each segment (κ) as a fraction of the segment length (L_s) (Table 2):

$$\kappa = \frac{\sqrt{I_{cm}/m_s}}{L_s} \quad (3)$$

These procedures allowed the segment masses, centers of mass, and moments of inertia to be estimated for the experimental animals using measures of body mass and segment lengths.

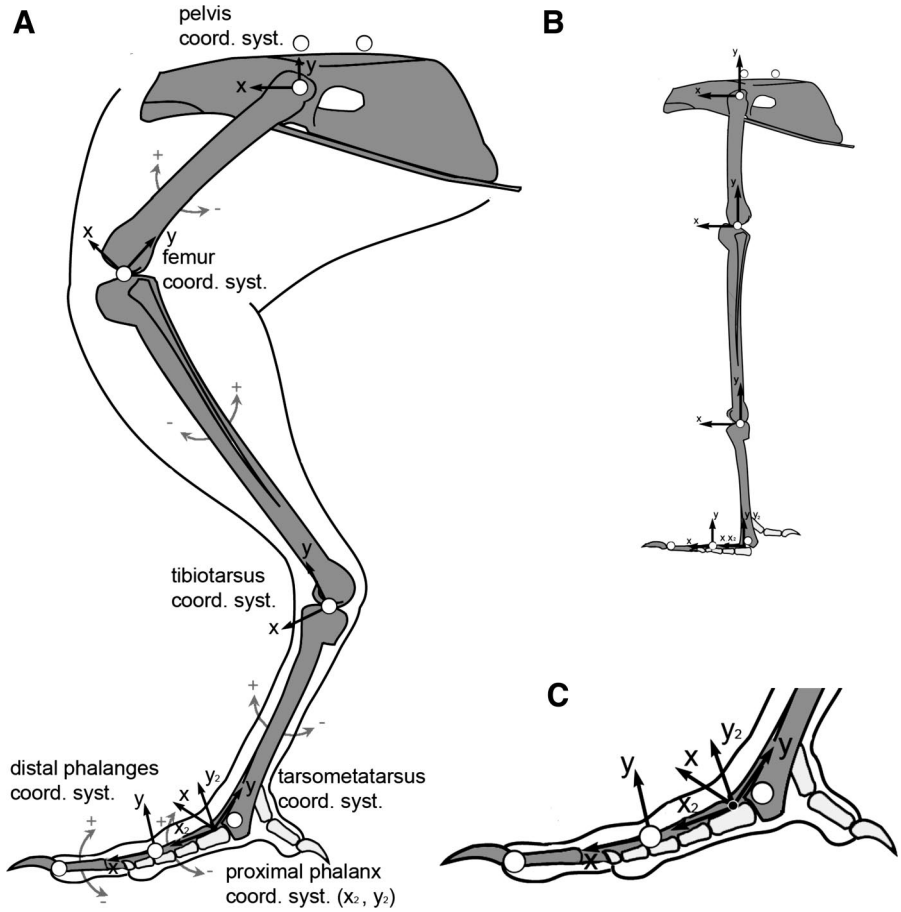

Fig. 1. *A*: illustration of segment markers and segment coordinate systems (SCS; dark arrows). The open circles represent retro-reflective markers attached to the limb. The shaded curved arrows represent positive and negative joint angle and moment directions. Note, the knee marker was placed on the approximate location of the knee center, but was only used for visual aid. The knee center was computed from the hip and ankle markers and segment lengths (see text). The distal tarsometatarsus marker was placed on the lateral base of the tarsometatarsus (LMB). The metatarso-phalangeal joint center (origin of the tarsometatarsus SCS) was computed from the LMB marker and the ankle marker (see Table 2). The distal and proximal phalanx markers were placed on digit III. Digit IV and the hallux are a lighter shade for clarity. *B*: illustration of the limb in a neutral posture where all joint angles are set to 0°. *C*: close-up of the segment coordinate systems of the tarsometatarsus and phalanx segments.

Inverse Dynamic Modeling

Standard two-dimensional inverse dynamic modeling was used to compute the net moments and mechanical power at the major hindlimb joints throughout limb swing following winter (62). The major hindlimb joints of the bird were marked with small retro-reflective markers (5-mm diameter; Fig. 1). These included the hip, knee, ankle, tarsometatarso-phalangeal (TMP), and interphalangeal (IP) joints. These markers were used to represent the joint centers of rotation, with the exception of the knee and TMP markers. Because skin movement causes the knee marker to move considerably, the knee's center of rotation was redefined as the intersection of the femur and tibiotarsus and was calculated from the length of these segments and the location of the hip and ankle joint centers. The necessity of this calculation of the knee center was verified by comparing trials using calculated and digitized knee joint locations. This comparison revealed large discrepancies in joint angles and angular excursion (up to 15° at both the knee and hip), as well as differences in computed limb-swing efficiencies (up to 15% difference). Because the TMP marker cannot be placed directly over the joint center, a spatial transformation (based on the anatomical specimens) was applied to locate the joint center throughout the stride (see Table 2 for description). The axis of the pelvis was determined by securing a lightweight foam-board block fit with two retro-reflective markers to the bird's synsacrum (Fig. 1). Feathers surrounding the bird's back and limb joints were removed to improve the visibility of the limb markers.

The animals were videoed in sagittal view walking and running on a motorized treadmill at four speeds (0.5, 1.0, 1.5, and 2.4 m/s) using high-speed video recordings (NAC-1000, 500-Hz field rate; NAC Image Technology, Simi Valley, CA). The 0.5-, 1.5-, and 2.4-m/s conditions were chosen because existing experimental data for limb-swing energy use exist at these speeds (14, 35, 49). The 1.0-m/s condition was included to assess the efficiency at a speed close to the animals walk-run transition speed (21).

The video from the NAC was converted to digital video (720 × 480 pixels) using an analog-to-digital converter (Canopus ADVC 55, Kobe, Japan). The digital video was then de-interlaced (JES Deinterlacer, Jan E. Schotsman, http://www.xs4all.nl/~jeschot/home.html) to recover the 500-Hz field rate of the NAC-1000. The de-interlaced frames were imported into ImageJ (Wayne Rasband, http://rsb.info.nih.gov/ij/). The imported video was first redimensioned to 720 × 528 pixels, which compensates for the rectangular aspect ratio of digital video pixels, and thresholded, which allowed the markers to be autotracked using the Mtrak2 plug-in (Nico Stuurman, University of California, San Diego, CA; http://valelab.ucsf.edu/~nico/IJplugins/MTrack2.html). This plug-in generated *x-y* pixel coordinate data for the joint and pelvis markers. In subsequent analyses of the filtered

Table 2. *Segment coordinate system definitions and segment anatomical properties*

Segment	SCS Definition	SCS Points	Segment Mass (Fraction Body Mass)	Radius of Gyration (Fraction Segment Length)	COM Position (Location in SCS; Fraction Segment Length)
Pelvis/body	origin: hip *x*: caudal pelvis → cranial pelvis *y*: (dorsal +)	distal pelvis: marker proximal pelvis: marker hip: marker	0.631	0.347	*x*: 0.178 *y*: −0.151
Femur	origin: knee *y*: knee → hip *x*: (anterior +)	hip: marker knee: computed*	0.0625	0.437	*x*: −0.0428 *y*: 0.589
Tibiotarsus	origin: ankle *y*: ankle → knee *x*: (anterior +)	ankle: marker knee: computed*	0.0492	0.294	*x*: 0.0015 *y*: 0.657
Tarsometatarsus	origin: TMP† *y*: TMP → ankle *x*: (anterior +)	ankle: marker TMP: computed†	0.0082	0.371	*x*: −0.0300 *y*: 0.525
Proximal phalanx	origin: TMP *x*: TMP → IP *y*: (cranial +)	TMP: computed† IP: marker	0.0051	0.490	*x*: 0.598 *y*: −0.243
Distal phalanx	origin: IP *x*: IP → claw *y*: (cranial +)	IP: marker claw: marker	0.0011	0.400	*x*: 0.587 *y*: 0.0057

For each segment coordinate system (SCS), the first axis is described by the arrow symbol (→), where the positive (+) direction is in the direction of the arrow. The second axis is perpendicular to the first. *The knee joint center is located by computing the intersection of the femur and tibiotarsus from the length of these segments measured on the experimental animal and the digitized hip and ankle joint markers. †The tarsometatarso-phalangeal (TMP) joint center is located from a coordinate system constructed from the ankle joint marker and a marker on the lateral base of the tarsometatarsus (LMB): origin: LMB; *y*: LMB → ankle; *x*: perpendicular (positive anterior). The location of the TMP center in this coordinate system expressed as a fraction of the tarsometatarsus length is *x* 0.0121, *y* 0.0811. IP, interphalangeal; COM, center of mass.

trajectories, units of pixels were converted to meters using the distance between the TMP and ankle markers measured on the animal and the average distance in pixels for this segment as it appeared on the video, thus mitigating the problem of parallax error resulting from the animal moving at different lateral positions on the treadmill.

Marker trajectory data were input into a custom-written procedure implemented in MATLAB (The Mathworks, Natick, MA) to compute joint angles, moments, power, and work using inverse dynamics. The MATLAB procedure was tested using benchmark input data for human locomotion (62). Coordinate data were low-pass filtered using a fourth-order, double-pass Butterworth filter. The cutoff frequency was determined separately for each *x*- and *y*-coordinate based on the residual analysis between filtered and unfiltered data (62). Cutoff frequencies were ~20 Hz and varied minimally between markers or animals.

Joint angles were computed as the angle between the *y*-axes of adjacent SCS. At the hip, knee, and ankle, flexion is represented by increasing angles and extension by decreasing angles. At the TMP and IP joints, increasing angles designate digital extension, and decreasing angles designate digital flexion. Zero-degree joint angles are defined as in Fig. 1*B*. Note that these joint angle conventions differ from some previous studies of avian locomotion (e.g., Refs. 20, 28) in that the sign of the angle in relation to flexion and extension is reversed. The sign convention adopted here is consistent with many human inverse dynamics studies and was adopted to allow consistency with the sign of the net joint moments, as defined below, and for the angular velocities and moments opposing gravity to all have the same sign (−, negative).

The net internal (muscle) moment at the proximal joint of each segment was computed by solving the equation:

$$M_p = I_{cm}\alpha - M_d - M_{r_{dx}} - M_{r_{px}} - M_{r_{dy}} - M_{r_{py}} \quad (4)$$

where M_p is the segment's proximal net joint moment (Nm), α is the angular acceleration of the segment (rad/s^2), M_d is the net joint moment acting on the segment at the distal joint, $M_{r_{dx}}$ and $M_{r_{px}}$ are the moments (Nm) generated by the *x*-component of the distal and proximal joint reaction forces about the segment center of mass, respectively, and $M_{r_{dy}}$ and $M_{r_{py}}$ are the moments (Nm) generated by the *y*-component of the distal and proximal joint reaction forces about the segment center of mass, respectively. Joint reaction forces were computed as:

$$F_{px} = (m_s \cdot a_x) - F_{dx} \quad (5)$$

$$F_{py} = (m_s \cdot a_y) + (m_s \cdot g) - F_{dy} \quad (6)$$

where F_{px} and F_{dx} are the *x*-component of the segment's proximal and distal joint reaction forces (N), respectively; F_{py} and F_{dy} are the *y*-component of the segment's proximal and distal joint reaction forces (N), respectively; and a_x and a_y are the accelerations of the segment center of mass in the *x*- and *y*-direction, respectively (m/s^2). The distal reaction force was equal to zero for the most distal segment. For all other segments, the distal joint reaction force was equal but opposite to the proximal joint reaction force at the adjacent segment.

Joint power was computed as:

$$P_j = M_p \cdot \omega_j \quad (7)$$

Where P_j is power (W), and ω_j is the joint angular velocity (rad/s). Positive joint work was computed at each joint by integrating the positive values of joint power over limb swing:

$$W_{j_i}^{+} = \int_{t_{sw1}}^{t_{sw2}} P_{j_i}^{+} dt \quad (8)$$

where $W_{j_i}^{+}$ is the positive work at the *i*th joint (J); $P_{j_i}^{+}$ is the positive power at the *i*th joint; t_{sw1} and t_{sw2} are the start and end of swing, respectively. The total positive work during limb swing (W_{sw}^{+}) was computed over one stride by summing the work from each joint and multiplying by 2 to represent both limbs:

$$W_{sw}^{+} = \left(\sum_{i=1}^{N} W_{j_i}^{+} \right) \cdot 2 \quad (9)$$

Previous studies demonstrate that only a single ankle flexor muscle, the tibialis cranialis, is active during the ankle flexion phase in early swing (35). The tibialis cranialis has two heads: the major head (comprising ~70% of the muscle mass) originates on the tibiotarsus, and a second small head originates on the femur, crossing anterior to

the knee joint. Assuming the tibialis cranialis is the only muscle responsible for ankle flexion, we estimated the positive mechanical work of this muscle by integrating the positive values of ankle joint power over the duration of the limb swing where an ankle flexion moment is present (Fig. 2). The duration of the ankle flexion moment in early swing corresponds to the time when the muscle is active, as determined by EMG (unpublished observations). We multiplied the tibialis cranialis mechanical work value by 2 to represent both the left and right limbs.

Efficiency Estimates

The metabolic rate of the muscles active during the swing phase of walking and running guinea fowl as a percent of the total metabolic rate of the leg muscles (Table 1) has been established in a series of studies integrating leg muscle blood flow measurements and whole body oxygen consumption (13, 14, 35, 49). These studies demonstrate that the limb-swing muscles consume between 22 and 27% of the increase in metabolic cost above rest during walking and running, depending on the assumptions about one large muscle known to be active in both limb swing and stance. This fractional cost of limb swing is constant over the range of locomotor speeds encompassing their aerobic scope. Based on these studies, we estimated the mass-specific metabolic rate of limb swing ($\dot{E}_{sw}$; W/kg) to be 25% of the net mass-specific metabolic rate after subtracting the metabolic rate during rest. We estimated the mass-specific net organismal metabolic rate of locomotion using data from Ellerby et al. (12) and the blood flow studies cited above. Three of the five experimental animals used here also had metabolic rates measured directly.

We also estimated the metabolic rate of the tibialis cranialis muscle over the four speed conditions. The metabolic rate of this muscle has been determined in the blood flow studies performed by Marsh and colleagues (14, 35, 49) and exhibits a constant fractional contribution to the metabolic cost of locomotion across walking and running speeds. Based on these previous studies, we estimated the metabolic rate of the tibialis cranialis ($\dot{E}_{tc}$) using a value of 8% of the net whole body metabolic rate. This value represents the average percentage of the total blood flow that is attributed to the tibialis cranialis muscle based on previous studies on guinea fowl (14, 35, 49).

To calculate the mechanical efficiency of the limb swing, we first calculated the total body mass-specific positive mechanical power of the limb swing ((P^{+}_{sw}), W/kg) by dividing the total positive mechanical work of the limb swing (*Eq. 9*) by the stride time (s) and body mass (kg). The η^{+}_{sw} was subsequently computed as:

$$\eta^{+}_{sw} = \frac{P^{+}_{sw}}{\dot{E}_{sw}} \cdot 100 \qquad (10)$$

where η^{+}_{sw} is mechanical efficiency, expressed in percent.

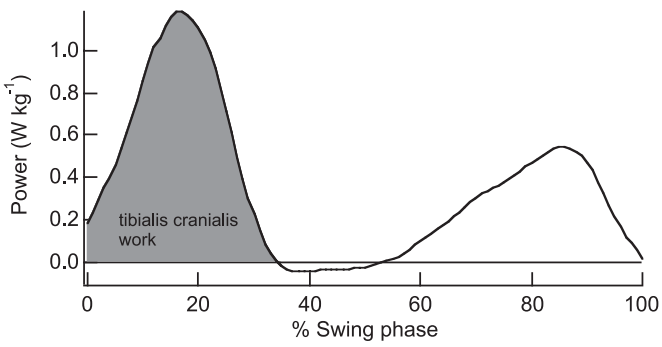

Fig. 2. Example of tibialis cranialis work output during ankle flexion. The work performed by the muscle is estimated by integrating the joint power curve over the duration of the limb swing where a net ankle flexion moment is present.

Because metabolic energy is also required for absorbing mechanical energy (negative mechanical work), we also computed an absolute mechanical efficiency for the positive mechanical work of swinging the limb by removing the estimated metabolic energy required for mechanical energy absorption. This was done by assuming a mechanical efficiency of energy absorption (η^{abs}_{sw}) of −120% (5, 34):

$$\eta^{abs}_{sw} = \frac{P^{+}_{sw}}{\dot{E}_{sw} - \left(\frac{P^{-}_{sw}}{-1.2}\right)} \cdot 100 \qquad (11)$$

where P^{-}_{sw} is the total body mass-specific negative mechanical power of the limb swing.

The total body mass-specific mechanical power of the tibialis cranialis (P_{tc}, W/kg) was calculated by dividing the total positive body mass-specific mechanical work of the tibialis cranialis by the stride time (s). Mechanical efficiency of the tibialis cranialis (η^{+}_{tc}) was subsequently estimated as:

$$\eta^{+}_{tc} = \frac{P_{tc}}{\dot{E}_{tc}} \cdot 100 \qquad (12)$$

RESULTS

Joint Angles, Moments, and Power

The angle-moment-power relationships at the hindlimb joints were generally consistent across the walking and running speeds and differed primarily in magnitude. Thus an example of angle, moment, and power data are presented for the 1.5-m/s condition, an intermediate running speed for guinea fowl (Fig. 3).

The hip undergoes rapid flexion during the first half of limb swing. During the first 40% of the limb swing, hip flexion occurs when there is a net flexion moment, resulting in a prominent burst of positive mechanical power at the joint. During midswing (40–80%), the hip remains static with little joint excursion (at faster speed, the hip undergoes more extension) and does so passively under negligible net moment and power. The later part of the limb swing is characterized by modest hip extension in conjunction with a net extension joint moment, thus resulting in a second positive power burst.

The knee undergoes flexion for the first 40% of limb swing. Knee flexion occurs primarily under the control of a net extension moment, resulting in negative power generated at the joint. The last 60% of limb swing is characterized by knee extension. Knee extension during midswing occurs passively, whereas, at the end of limb swing (80–100%), knee extension continues in the presence of a net flexion moment, resulting in negative joint power.

The ankle exhibits a simple flexion-extension cycle over the duration of the limb swing. The ankle flexion and extension is accompanied by positive net flexion and extension moments, respectively, resulting in positive power being generated at the joint, primarily at the beginning and the end of swing.

The TMP joint and the IP joints undergo rapid digital flexion following toe-off. After midswing, these joints undergo digital extension. Digital flexion during early limb swing is under control of a small net digital extension moment, resulting in a burst of negative joint power. During the remainder of the limb swing, the moments at the TMP and IP joints are negligible, resulting in minimal joint power.

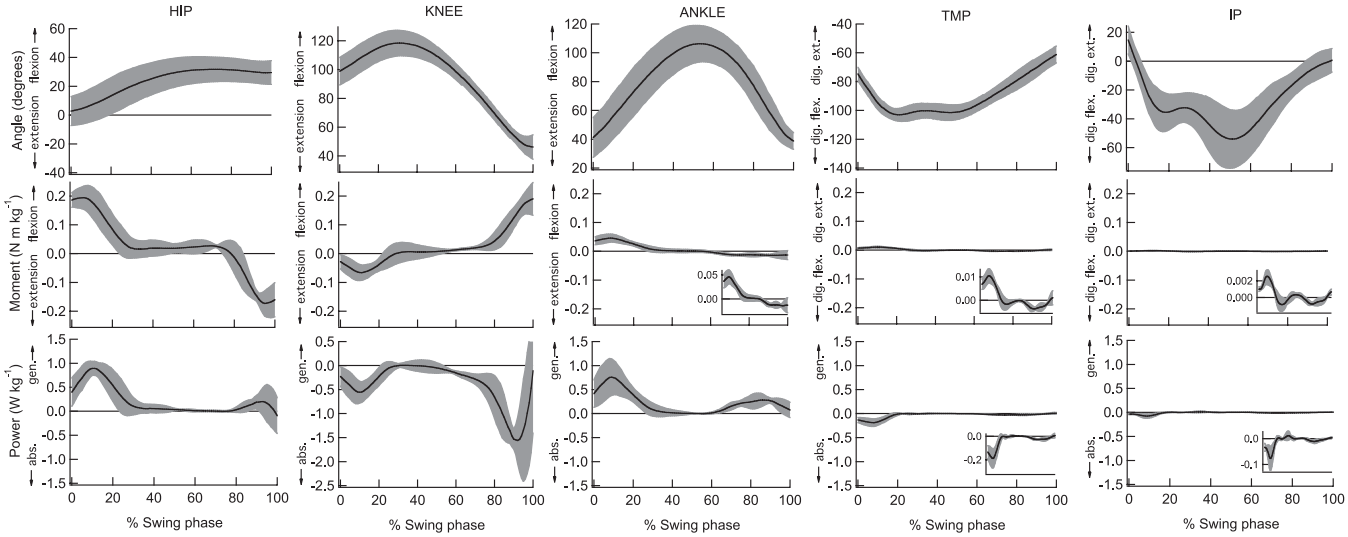

Fig. 3. Joint angle, moment, and power traces for the major hindlimb joints over limb swing during running (1.5 m/s). The traces represent mean data (±SD; shaded region). Joint flexion is represented by an increase in the joint angles, and joint extension is represented by decreasing angles, except for the tarsometatarso-phalangeal (TMP) and interphalangeal (IP) joints, where increasing angles represent digital extension, and decreasing angles represent digital flexion. Joint moments are internal (muscle) moments. Net flexion joint moments are positive, and net extension moments are negative (digital extension moments are positive, and digital flexion moments are negative). *Inset* graphs are included to illustrate the shape of the traces at the joints where moment and power values are small. Faster and slower speeds exhibit similar patterns, differing primarily in magnitude. gen, Power generation; abs, power absorption.

Mechanical Work, Power, and Efficiency

The mechanical work and power of the limb swing is distributed unevenly across the hindlimb joints (Fig. 3, Table 3). The hip and ankle perform the majority of positive work of limb swing, whereas the knee absorbs work throughout swing (negative work). The TMP and IP joints also primarily absorb work and only provide a very small component of the overall work of limb swing. The estimated mechanical work and power of the tibialis cranialis (the work of ankle flexion in early swing) accounts for nearly one-third of the total positive limb swing work and the average limb swing positive mechanical power (summed across all joints) at the 1.0- to 2.4-m/s speed conditions (Table 4). This value is commensurate with this muscle's contribution to the total limb swing energy use (~30%). At 0.5 m/s, this muscle contributed to ~50% of the total positive limb swing power, although measurements were more variable at this speed.

The average limb-swing positive mechanical power (total positive work at each joint, summed across joints) increased from 0.031 W/kg body mass at 0.5 m/s to 1.08 W/kg body mass at 2.4 m/s, and the relation of power and speed was fit by a power function (Fig. 4*A*, Table 4). The efficiency of limb swing, as assessed from an estimate of the metabolic energy use of active limb-swing muscles, increased linearly from 2.56% at 0.5 m/s to 17.2% at 2.4 m/s (Fig. 4*B*). When the estimated metabolic cost of absorbing energy was taken into account, the efficiency of limb swing increased to 3.17% at 0.5 m/s and 20.0% at 2.4 m/s (Fig. 4*B*).

The average mechanical power attributed to the tibialis cranialis muscle during ankle flexion (during the first 40% of limb swing) increased with speed from 0.02 W/kg body mass at 0.5 m/s to 0.29 W/kg body mass at 2.4 m/s (Fig. 5*A*, Table 4). The increase in mechanical power of the tibialis cranialis was fit with a power function. The estimated mechanical

Table 3. *Body mass-specific mechanical work and average mechanical power during running at 1.5 m/s*

	W^+, J/kg (±SE × 10^{-2})	W^-, J/kg (±SE × 10^{-2})	P^+, W/kg (±SE × 10^{-2})	P^-, W/kg (±SE × 10^{-2})
Joint (W_j^+, W_j^-)				
Hip	8.42±0.58	−0.73±0.03		
Knee	0.85±0.59	−15.0±0.65		
Ankle	8.22±0.79	−0.25±0.12		
TMP	0.07±0.03	−1.25±0.16		
IP	0.08±0.03	−0.42±0.08		
Total limb (W_{sw}^+, W_{sw}^-, P_{sw}^+, P_{sw}^-)	17.6±0.73	−17.6±0.78	43.5±1.38	−43.6±1.32
Tibialis cranialis (W_{tc}^+ and P_{tc}^+)	5.57±0.70		13.7±1.78	

Values are means ± SE ×10^{-2}. Shown are the distribution of body mass-specific mechanical work between the major hindlimb joints, body mass-specific work and average power of the entire limb, and estimated body mass-specific work and average power of the tibialis cranialis muscle. The work and power values represent the sum of both limbs. W^+ and W^-, positive and negative work, respectively; P^+ and P^-, positive and negative power, respectively; W_j^+ and W_j^-: positive and negative joint work, respectively; W_{tc}^+, positive work of the tibialis cranialis muscle; W_{sw}^+ and W_{sw}^-: total positive and negative work of the entire limb swing, respectively; P_{sw}^+ and P_{sw}^-: positive and negative average limb swing power, respectively; P_{tc}^+, average positive power of the tibialis cranialis muscle.

Table 4. *Body mass-specific mechanical work and average power of limb swing and the tibialis cranialis muscle at each speed condition*

Speed Condition, m/s	W^{+}_{sw}, J/kg	W^{-}_{sw}, J/kg	P^{+}_{sw}, W/kg	P^{-}_{sw}, W/kg	W^{+}_{tc}, J/kg	P^{+}_{tc}, W/kg
0.5	2.41±0.75	−3.41±1.14	3.07±1.01	−4.30±1.59	1.21±0.16	1.70±0.28
1.0	9.99±1.43	−10.6±1.31	21.3±3.51	−22.6±3.24	3.10±0.25	6.54±0.68
1.5	17.6±0.73	−17.6±0.78	43.5±1.38	−43.6±1.32	5.57±0.70	13.7±1.78
2.4	35.6±1.09	−33.7±1.23	108±4.45	−103±4.67	9.57±1.17	29.1±3.75

Values are means ±SE $\times 10^{-2}$. The work and power values represent the sum of both limbs.

efficiency of ankle flexion produced by the tibialis cranialis muscle increased linearly from 2.85% at 0.5 m/s to 14.8% at 2.4 m/s (Fig. 5*B*).

DISCUSSION

We asked whether mechanical work, measured as net joint work using inverse dynamics, is a major determinant of energy use by limb-swing muscles. Although this measure of work is not the only one possible, evaluating this question is important, because net mechanical work is a quantity that can be estimated without invasive studies. If this measure of work were found to be a reliable indicator of metabolic cost, it would bolster human studies that attempt to relate variation in mechanical work to variation in metabolic energy (see, for example, Refs. 18, 38, 45). However, we found that, in terms of producing net mechanical work, both the overall efficiency of the limb swing and the estimated efficiency of the tibialis cranialis muscle increased markedly from walking to fast running. The measured efficiencies are also below the usually accepted maximum efficiency of muscle, except at the fastest speeds recorded. These findings do not support the hypothesis that net joint work is the major determinant of limb-swing energy use across all speeds and warn against making simple predictions of energy use during limb swing based on joint mechanical work, particularly for walking.

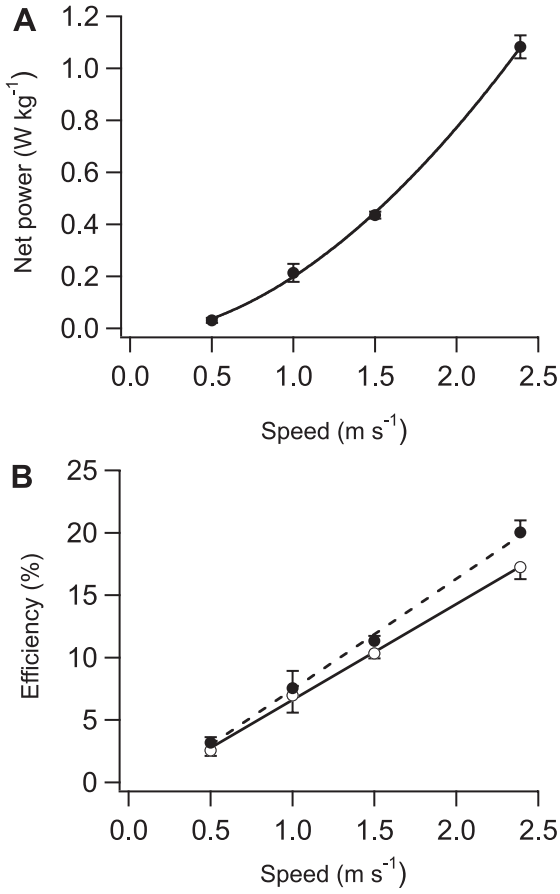

Fig. 4. *A*: body mass-specific net mechanical power of limb swing as a function of speed (v) (±SE). Average mechanical power was fit with a power function ($P_{sw} = -0.03 + 0.23v^{1.83}$, where v is in m/s). *B*: mechanical efficiency of limb swing as a function of speed (±SE). Positive efficiency (solid line) and absolute efficiency (after removing the estimated cost of absorbing work; dashed line) increase linearly (mechanical efficiency $\eta^{+}_{sw} = 7.68v - 1.07$, $r^2 = 0.99$, and mechanical efficiency of energy absorption $\eta^{abs}_{sw} = 8.87v - 1.43$, $r^2 = 0.99$, respectively, where v is in m/s).

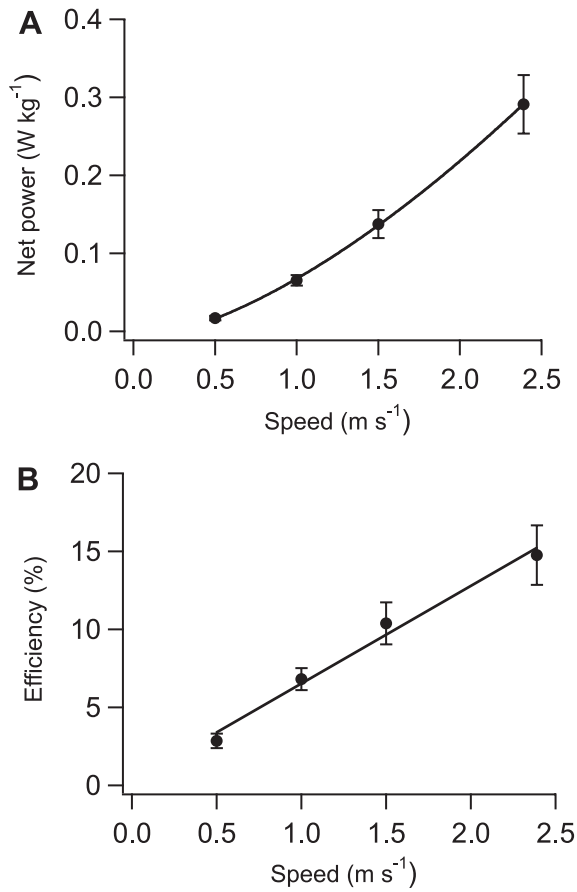

Fig. 5. *A*: body mass-specific net mechanical power estimated for the tibialis cranialis muscle as a function of speed (±SE). The average tibialis cranialis mechanical power was fit with a power function ($P_{tc} = -0.01 + 0.08v^{1.56}$, where v is in m/s). *B*: mechanical efficiency of the tibialis cranialis muscle as a function of speed (±SE). Efficiency increases linearly ($\eta^{+}_{tc} = 6.25v + 0.27$, $r^2 = 0.99$, where v is in m/s).

Efficiency Expected of Muscles Producing Mechanical Work

What is the appropriate value of maximal muscle efficiency to which our values should be compared? The denominator in the efficiencies we have measured is based on the energy equivalent of oxygen consumption (20.1 J/ml O_2; Ref. 53), and thus our efficiencies should be compared with measures of overall muscle efficiency that include the efficiency of the oxidative production of ATP. The maximal overall efficiency of guinea fowl muscles is not known, but a value of 20–25% is a reasonable estimate, based on what is known from other animals. The literature on efficiencies is limited, but it is clear that human muscle operating in vivo has a maximum overall efficiency of 25–30% (e.g., Ref. 17). Guinea fowl (1.5 kg) are considerably smaller than humans, and maximal efficiency may be reduced in the muscles of smaller animals operating at higher contractile frequency. Rat (body mass < 0.5 kg) muscle has an overall efficiency of ~20% based on in vitro measures of oxygen consumption in isolated fast-twitch extensor digitorum longus muscle (25) and in situ measures of metabolite concentrations (1). (Conversion of the metabolite data to efficiency assumes a value of 55 kJ/mol for the free energy of ATP hydrolysis and an efficiency of oxidative ATP production of 60%.) Efficiency is reduced when muscles operate under suboptimal conditions, e.g., nonoptimal relative shortening velocity (V/V_{max}) for a particular fiber type. However, the low efficiency we have estimated at low speeds seems unlikely to have been caused by operating at a low V/V_{max}. The efficiency vs. shortening speed relation for isolated muscle is quite flat at low shortening speeds (25, 31). Also, guinea fowl, like humans, have an array of fiber types in their leg muscles (32) that can allow the muscles to operate closer to their optimal V/V_{max} over a range of shortening speed. In humans, efficiency changes little over a broad range of operating frequencies when the main task is producing mechanical work (17, 19).

Therefore, compared with an expected maximal efficiency of 20–25%, the mechanical efficiency of the summed swing phase muscles at the fastest speed (17%, or 20% considering the cost of absorbing work) seems indicative of muscles using energy mostly to perform positive mechanical work. However, the low-efficiency values during walking and slower running speeds suggest that limb-swing energy use at these lower speeds is dictated in large part by mechanical processes other than net joint work.

Mechanical Work as a Determinant of the Tibialis Cranialis Energy Use

One potential problem of using work summed across all joints is that links to muscle use can be obscured by variable function of a number of muscles across several joints. An advantage of using an inverse dynamic approach to compute ankle joint work in the present study is the ability to estimate the mechanical work of a single muscle, the tibialis cranialis. This estimation is possible because the tibialis cranialis is the only muscle recruited for ankle flexion during the first half of limb swing (35) and is thus responsible for providing the computed net work in ankle flexion. Combined with muscle-specific blood flow measurements, these data permit (to the best of our knowledge) the first estimate of the in vivo efficiency of an individual muscle during animal locomotion.

Interestingly, the pattern of mechanical work and efficiency observed for the tibialis cranialis mirrors that of the total limb swing; the slope of mechanical work vs. speed increases with increasing speed, and efficiency increases from 3% (walking) to 15% (fast running). Like those of the total limb swing, these data indicate that (except possibly at the fastest speed) the mechanical work performed during ankle flexion is not strongly associated with the metabolic energy used by the tibialis cranialis muscle to perform this motion. It is interesting that the pattern observed for a single joint and muscle matches so closely that of the total limb swing. The tibialis cranialis accounts for ~30% of the total limb-swing energy expenditure, more than any other limb-swing muscle (35, 49). The data on the tibialis cranialis suggest that factors determining the dissociation between net joint work and muscle metabolic energy use are consistent across the muscles operating at the different joints. Although these factors remain unclear, the ability to estimate the mechanics and energetics of an individual muscle strengthens our conclusion that net joint work is not the only major determinant of limb-swing energy use when considered across running speed.

Comparison to Past Studies Linking Mechanical Work and Limb-Swing Energy Use

Strong evidence that mechanical work is a major determinant of energy cost would be provided, if metabolic rate increased proportionately with increases in the mechanical work performed, and efficiency was constant and appropriate for muscle working under near optimal conditions. This reasoning provided the underpinnings of a pioneering set of papers from the laboratory of C. R. Taylor (16, 26, 27, 57). These investigators examined variation in metabolic and mechanical power with speed in a variety of animals of different body size. They concluded that mechanical work is not the major determinant of the overall energy use during legged locomotion, leading to the alternate hypothesis that the force required to support the body during stance dictates metabolic cost. The view that mechanical work is not linked to energy use during locomotion has generally been upheld (29, 44). However, putting aside the determinants of energy use in stance, these studies did not address the relation of mechanics and energetics during limb swing because they did not partition the mechanical work of limb swing and stance nor the metabolic cost of limb swing, which was assumed to be negligible.

Because the most obvious mechanical function occurring during limb swing is the acceleration of the limb segments, the link between energy use and limb-swing work has been examined in a number of previous studies. A major approach has been to alter the mechanical work done and examine the effect on energy use. Increases in mechanical work have been produced by loading the distal limb both in humans (6, 36, 37, 48) and other species, including guinea fowl (36, 55). Loading the distal limb with added mass increases the mechanical work required to swing the limb and also increases the organismal metabolic energy expenditure, which suggests a link between the mechanical work of limb swing and metabolic energy use (6, 36, 37, 42, 48). In guinea fowl, the increase in metabolic cost after limb loading is distributed among swing- and stance-phase muscles in proportion to the division of the increased work required to accelerate the added mass, demonstrating a

strong correlation between the increase in mechanical work and the increase in limb-swing energy use (14). An alternate approach is to decease the mechanical work to accelerate the limb in early swing by providing a swing-assist device (23, 41). These studies indicate a decrease in organismal energy use and thus also suggest an association of limb-swing energy cost and mechanical work, although the quantitative relation between these variables was not specified.

Interestingly, the present study does not appear to share an equally strong association between limb-swing metabolic energy use and mechanical work when examined across the range of speeds tested. Whereas limb-swing metabolic energy use increases linearly with speed, the slope of mechanical power vs. speed increases substantially over the range of speeds studied. This discrepancy between the effect of speed on metabolic cost and mechanical work rate results in a large increase in mechanical efficiency from walking (2.5%) to fast running (17%).

Nevertheless, leaving aside the substantial technical differences among the studies (e.g., in how mechanical work was quantified), the data presented here and these past data are reasonably consistent. Taken together, they suggest the hypothesis that mechanical work during limb swing is a more important determinant of energy cost when the rate of work output (power) is high than when it is low, as it is during unloaded walking, especially at slow speed. The apparent efficiencies of performing the extra work of accelerating the limb load in guinea fowl (36) are higher across all speeds than those presented here, but the increases in work induced by limb loading are large compared with unloaded work, even during walking. Also, Marsh et al. (36) noted that the apparent efficiency increased with apeed as the work of accelerating the load also increased. In the swing-assist studies on humans, the assist device provides the mechanical work required to accelerate the limb in early swing. This device can, therefore, be expected to decrease limb-swing energy use in proportion to the importance of mechanical work in determining limb-swing cost. The reduction in total energy use with the swing assist is larger during running (20%; Ref. 41) vs. walking (10%; Ref. 23), which again indicates that the mechanical work to accelerate the limb may be a larger factor in determining energy use at higher speeds and workloads.

Alternate Mechanical Determinants of Limb-swing Costs

If net mechanical work at the joints does not explain limb-swing energetics, what other mechanical functions explain limb-swing energy use across the animals' speed range? Two alternative and likely complementary explanations seem clear: *1*) muscle energy use is in part determined by the requirements for force production that are not tied to mechanical work output; and *2*) net joint work does not correspond to muscle work.

Cost of force production. Muscles consume energy not solely to produce mechanical work, but also to produce force, including when they contract isometrically and perform no muscle work. Proposing the cost of force as a clear alternative to the cost of work as a determinant of energy use is complicated by the fact that muscles produce force, when both producing and absorbing work, and thus in some sense all energy use in muscle is related to force production, albeit with a variable economy. The clearest alternative is provided by muscles contracting isometrically. Energy use in muscles functioning isometrically (or shortening very slowly) confounds efficiency estimates based on joint mechanics, from which individual muscle dynamics are difficult to deduce. The concept that locomotor cost is determined by muscle force, as opposed to mechanical work, has received considerable attention with regard to stance-phase cost. The production of muscle force, which is assumed to be proportional to the ground reaction force during stance, has been used to explain the metabolic cost of walking and running in humans and other terrestrial vertebrates (24, 30, 47). Force production, rather than mechanical work, has also been correlated with the metabolic cost of stationary one-legged limb-swing exercise in humans (10, 11).

The extent of isometric force production during limb swing in guinea fowl and the associated energy use remain ambiguous. During midswing, when joint rotations are small and when muscles can most plausibly operate close to isometrically, the net joint moments are negligible, indicating that no net muscle force is required. Muscles could, however, function isometrically and use energy in midswing by cocontracting against antagonists (for a diagram of the major swing-phase muscles and their percent contribution to the metabolic cost of limb swing, see Fig. 6). Furthermore, because the net joint moments during early and late swing are accompanied by significant power generation/absorption, for muscles to function isometrically during these periods would require substantial storage and release of elastic strain energy to explain the observed joint power. Given that many of the proximal limb-swing muscles are parallel fibered with little tendon (the primary source for elastic storage/release), isometric force production in these muscles during early and late swing appears unlikely.

The relation of muscle work and joint work. A second possible explanation for the lack of a proportional increase in mechanical work rate and energy cost with speed is that net joint work does not correspond to muscle work. Inverse dynamic analyses only estimate the net output of all forces crossing the joints (including both muscle forces and forces arising from other tissues, such as ligaments) and not the force and work done by individual muscles. Muscles may have functions requiring mechanical work in addition to the net mechanical work done in accelerating and decelerating the limb segments, as estimated by inverse dynamics, or alternatively the interacting dynamics of the limb may result in muscle work that is less than the net joint work. Additional positive muscle work could be required to rotate the joint against joint moments that oppose the measured net moment. Less muscle work could be required if elastically stored energy provides some of the limb-swing work, or if work is transferred by two joint muscles at points in the stride when work is positive at one joint and negative at an adjoining joint.

One well-known function of muscle that requires mechanical work above that which is measured from inverse dynamics is cocontraction of agonist and antagonist muscles. The positive work produced by the agonist muscle-tendon units is greater than the computed positive net joint work because they have to do work against cocontracting antagonist muscles in addition to accelerating the limb segment. The antagonist muscle, in

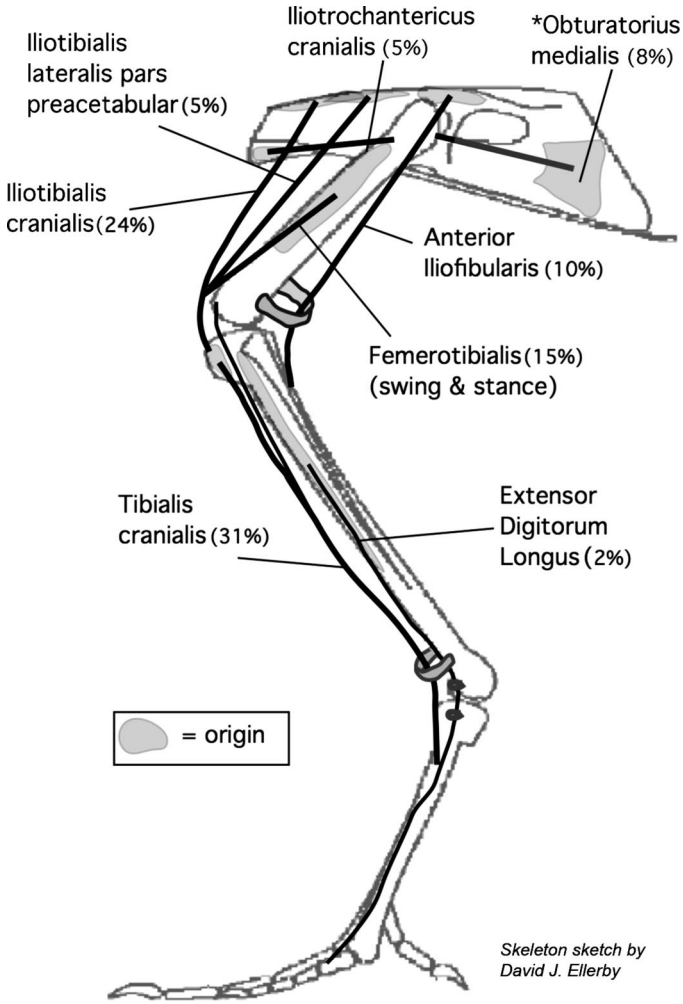

Fig. 6. The lines of action for the major limb-swing muscles and the approximate extent of their origins (shaded regions). The percent contribution of each muscle to the total limb-swing metabolic energy use is denoted in parentheses. Note that, during swing, the major knee flexor, the anterior iliofibularis, is opposed at the knee by the iliotibialis cranialis and the preacetabular portion of the iliotibialis lateralis, both of which serve as major hip flexors. *The obturatorius medialis originates on the medial surface of the pelvis.

this case, absorbs mechanical energy (negative work), a mechanical function also not measured in the inverse dynamic analysis. EMG data from limb-swing muscles show that significant cocontraction exists in guinea fowl, in particular across the knee joint (20, 35). Cocontraction also exists in human limb swing (22).

A second factor that is often overlooked in mechanical gait analyses that could lead to an underestimate of muscle work is the work required to stretch passive muscles and overcome the resistance in articular structures (passive joint moments). In humans, the magnitude of these passive joint moments are significant compared with the net joint moments during limb swing and are thought to result primarily from passive muscle force (33, 52, 59). Passive moments have both a dominant passive-elastic component and a dissipative component (15, 46). Both components may require additional muscle work, and passive-dissipative moments do not permit any exchange of useful mechanical energy.

Muscles thus function and consume energy not only to accelerate the limb segments during limb swing, but also to do mechanical work against both active and passive muscles that oppose the net joint moment. Accordingly, if our measurements of net mechanical work underestimate the total muscle work, it follows that the mechanical efficiency measurements underestimate the actual efficiency of muscle. Furthermore, if the amount of muscle work attributed to cocontraction and overcoming passive joint moments is constant across speed, these factors will help explain why our calculated efficiency values increase with faster running speed. In support of this hypothesis, data from passive joint moment experiment suggest that velocity-dependent effects are small (15, 64).

Elastic energy storage and release could result in an overestimate of muscle work during limb swing based on net joint work, if elastic energy stored in stance could be released in swing. Most of the major limb-swing muscles that consume large amounts of energy are proximal parallel-fascicled muscles, which seem ill suited to elastic energy storage. The exception is the pinnate tibialis cranialis muscle, which has a long tendon that could stretch and store energy. Presence of elastic energy storage/release in this tendon is suggested by a high peak power output during ankle flexion. The maximum muscle mass-specific power output based on our joint work measurements is 400 W/kg. Using data from turkey muscles (43), Henry et al. (28) have suggested 380 W/kg as a reasonable estimate of the peak isotonic power of guinea fowl muscle. Although this value is only slightly lower than the maximum value we recorded here, it assumes maximal recruitment of the muscle, and the birds in the present study were not running at maximum speed. Storage (and subsequent release) of elastic energy in the tibialis cranialis tendon could result either from shortening of the tibialis cranialis fibers during limb swing, or from the ankle extensors stretching the tendon in late stance, if the tibialis cranialis is activated at this time. EMG data suggest the majority of force in this muscle is produced during limb swing (35). However, if some force could also be produced before toe-off, while the ankle is extending, energy could be stored in the tendon while the tibialis cranialis fibers were isometric or lengthening. This function would be akin to the catapult mechanism described for the horse forelimb (61).

Energy transfer by two joint muscles generating simultaneous positive and negative work at adjoining joints could cause the positive muscle work to be less than positive net joint work summed across the individual joints (65). However, this transfer seems unlikely to be a major factor in guinea fowl, because most of the positive work occurs in early swing and most of the negative work occurs in late swing (Fig. 3). Some energy may be transferred between the knee and ankle joints in early swing via the small head of the tibialis cranialis muscle that crosses the knee, but the extent of this transfer requires knowledge of individual muscle mechanics.

Guinea Fowl as a Model for Human Locomotion

The ability to obtain experimental biomechanical and physiological data from guinea fowl locomotor muscles, and the fact that they are habitual bipeds, make these animals an attractive model for understanding both normal and dysfunc-

tional gait in humans. As a model, guinea fowl should ideally reflect the mechanics of locomotion in humans. It has been shown previously that stance-phase mechanics are similar in guinea fowl and humans, where the joints undergo a similar loading pattern in both species (8). In this study, we show that the similarity in joint loading between guinea fowl and humans also applies to limb swing. Both the joint angle, joint moment, and joint power profiles are remarkably similar between the two species, especially considering the difference in limb proportions and overall size (for representative human data see Refs. 39, 62).

To demonstrate more clearly the similarity in limb-swing joint mechanics, we have compiled plots of hip, knee, and ankle joint power in guinea fowl and humans normalized to their maximum power over the limb swing (Fig. 7). Joint powers, rather than joint moments, were chosen for comparison because they incorporate both joint moments and angles and, therefore, are a more robust indicator of mechanical similarity. Representative human joint powers from running (3 m/s) were obtained from Besier et al. (Ref. 4; and T. F. Besier, personal communication). Although there is a lag in the joint power traces at the hip and ankle, similar patterns of power generation and absorption are observed at each joint. Cross-correlation between human and guinea fowl joint power traces yield R values of 0.92, 0.88, and 0.83 at the ankle, knee, and hip, respectively (xcorr function using MATLAB 7, The MathWorks, Natick MA).

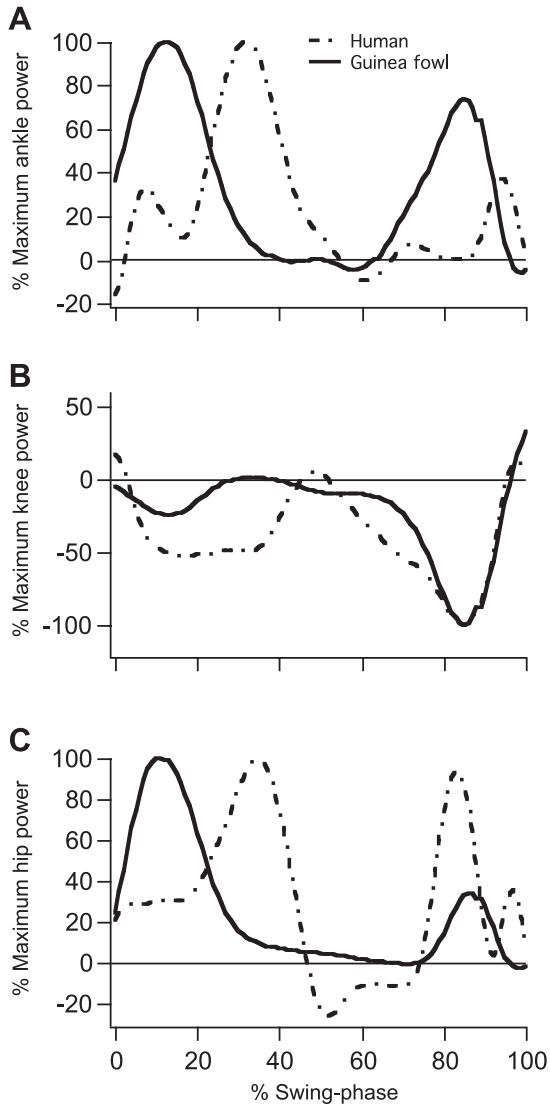

Fig. 7. Comparison of hip (*A*), knee (*B*), and ankle joint power (*C*) over limb swing in guinea fowl (solid lines) and humans (dotted-dashed lines). Guinea fowl data are from running at 1.5 m/s, and human data are from running at 3 m/s, an equivalent speed based on Froude number (21). Joint power is normalized to the maximum (minimum at the knee) power over limb swing. Joint powers exhibit similar patterns in both species, as represented by the strong cross-correlation between traces (R values of 0.83, 0.88, and 0.92 were computed for the hip, knee, and ankle traces, respectively).

These findings indicate that, despite their anatomical differences, guinea fowl are a useful model of bipedal gait and reinforces the applicability of the present study for understanding limb-swing mechanics and energetics in humans. In particular, the present study indicates that predicting limb-swing energy use in humans from mechanical measurements may not be reliable. Therefore, clinical studies aiming to understand variation in energy use should consider alternate diagnostic tools of limb-swing mechanics. Our findings can also help inform treatment of gait impairments and are of particular relevance to prosthetic limb design, where the relationship between prosthetic design, mechanical work, and limb-swing energy use is of central interest (48, 50). Our data suggest criteria other than reducing net mechanical work may be more important for the design of metabolically economical prostheses.

Conclusion

This study shows that net mechanical work at the joints is not a strong determinant of limb-swing muscle energy use across slow and moderate locomotor speed. Although the factors responsible for the poor association between mechanical and metabolic energy use remain unclear, our findings indicate that mechanical functions other than accelerating the limb segments determine limb-swing energy use. These functions may include isometric muscle force to redirect limb segments, as well as muscle work required to overcome cocontraction and passive joint moments. Exploring these alternate limb-swing muscle functions and their associated energy requirements will be essential for uncovering the mechanical determinants of limb-swing costs and can prove important for treatment of limb-swing impairments in humans. These studies will require methods that overcome the limitations of simple inverse dynamic analyses including the force distribution among individual muscles (including antagonist muscle forces), mechanical energy transfer via two-joint muscles, and energy storage/release in tendon. More complex modeling approaches (static and dynamic optimization) and direct in vivo measurements will prove valuable approaches.

ACKNOWLEDGMENTS

The authors thank Jennifer Carr, Peter Dimoulas, Havalee Henry, and Tom Hoogendyk for assistance in data collection, David Ellerby for the use of the bone images used in Figs. 1 and 6, and two anonymous reviewers for helpful comments and suggestions.

GRANTS

This work was supported by National Institute of Arthritis and Musculoskeletal and Skin Diseases Grant AR47337 and National Science Foundation Grant IOS-0542795 to R. L. Marsh.

REFERENCES

1. **Abbate F, De Ruiter CJ, Offringa C, Sargeant AJ, De Haan A.** In situ rat fast skeletal muscle is more efficient at submaximal than at maximal activation levels. *J Appl Physiol* 92: 2089–2096, 2002.
2. **Alexander RM.** *Animal Mechanics.* Oxford: Blackwell Scientific, 1983.
3. **Arnold AS, Thelen DG, Schwartz MH, Anderson FC, Delp SL.** Muscular coordination of knee motion during the terminal-swing phase of normal gait. *J Biomech* 40: 3314–3324, 2007.
4. **Besier TF, Lloyd DG, Ackland TR.** Muscle activation strategies at the knee during running and cutting maneuvers. *Med Sci Sports Exerc* 35: 119–127, 2003.
5. **Bigland-Ritchie B, Woods JJ.** Integrated electromyogram and oxygen uptake during positive and negative work. *J Physiol* 260: 267–277, 1976.
6. **Browning RC, Modica JR, Kram R, Goswami A.** The effects of adding mass to the legs on the energetics and biomechanics of walking. *Med Sci Sports Exerc* 39: 515–525, 2007.
7. **Collins S, Ruina A, Tedrake R, Wisse M.** Efficient bipedal robots based on passive-dynamic walkers. *Science* 307: 1082–1085, 2005.
8. **Daley MA, Biewener AA.** Muscle force-length dynamics during level versus incline locomotion: a comparison of in vivo performance of two guinea fowl ankle extensors. *J Exp Biol* 206: 2941–2958, 2003.
9. **Datta D, Heller B, Howitt J.** A comparative evaluation of oxygen consumption and gait pattern in amputees using Intelligent Prostheses and conventionally damped knee swing-phase control. *Clin Rehabil* 19: 398–403, 2005.
10. **Doke J, Donelan JM, Kuo AD.** Mechanics and energetics of swinging the human leg. *J Exp Biol* 208: 439–445, 2005.
11. **Doke J, Kuo AD.** Energetic cost of producing cyclic muscle force, rather than work, to swing the human leg. *J Exp Biol* 210: 2390–2398, 2007.
12. **Ellerby DJ, Cleary M, Marsh RL, Buchanan CI.** Measurement of maximum oxygen consumption in guinea fowl *Numida meleagris* indicates that birds and mammals display a similar diversity of aerobic scopes during running. *Physiol Biochem Zool* 76: 695–703, 2003.
13. **Ellerby DJ, Henry HT, Carr JA, Buchanan CI, Marsh RL.** Blood flow in guinea fowl *Numida meleagris* as an indicator of energy expenditure by individual muscles during walking and running. *J Physiol* 564: 631–648, 2005.
14. **Ellerby DJ, Marsh RL.** The energetic costs of trunk and distal-limb loading during walking and running in guinea fowl *Numida meleagris*. II. Muscle energy use as indicated by blood flow. *J Exp Biol* 209: 2064–2075, 2006.
15. **Esteki A, Mansour JM.** An experimentally based nonlinear viscoelastic model of joint passive moment. *J Biomech* 29: 443–450, 1996.
16. **Fedak MA, Heglund NC, Taylor CR.** Energetics and mechanics of terrestrial locomotion. II. Kinetic energy changes of the limbs and body as a function of speed and body size in birds and mammals. *J Exp Biol* 79: 23–40, 1982.
17. **Ferguson RA, Ball D, Krustrup P, Aagaard P, Kjaer M, Sargeant AJ, Hellsten Y, Bangsbo J.** Muscle oxygen uptake and energy turnover during dynamic exercise at different contraction frequencies in humans. *J Physiol* 536: 261–271, 2001.
18. **Foerster SA, Bagley AM, Mote CD Jr, Skinner HB.** The prediction of metabolic energy expenditure during gait from mechanical energy of the limb: a preliminary study. *J Rehabil Res Dev* 32: 128–134, 1995.
19. **Gaesser GA, Brooks GA.** Muscular efficiency during steady-rate exercise: effects of speed and work rate. *J Appl Physiol* 38: 1132–1139, 1975.
20. **Gatesy SM.** Guineafowl hind limb function. I. Cineradiographic analysis and speed effects. *J Morphol* 240: 115–125, 1999.
21. **Gatesy SM, Biewener AA.** Bipedal locomotion effects of speed size and limb posture in birds and humans. *J Zool Lond* 224: 127–148, 1991.
22. **Gazendam MG, Hof AL.** Averaged EMG profiles in jogging and running at different speeds. *Gait Posture* 25: 604–614, 2007.
23. **Gottschall JS, Kram R.** Energy cost and muscular activity required for propulsion during walking. *J Appl Physiol* 94: 1766–1772, 2003.
24. **Griffin TM, Roberts TJ, Kram R.** Metabolic cost of generating muscular force in human walking: insights from load-carrying and speed experiments. *J Appl Physiol* 95: 172–183, 2003.
25. **Heglund NC, Cavagna GA.** Mechanical work, oxygen consumption, and efficiency in isolated frog and rat muscle. *Am J Physiol Cell Physiol* 253: C22–C29, 1987.
26. **Heglund NC, Cavagna GA, Taylor CR.** Energetics and mechanics of terrestrial locomotion. III. Energy changes of the centre of mass as a function of speed and body size in birds and mammals. *J Exp Biol* 79: 41–56, 1982.
27. **Heglund NC, Fedak MA, Taylor CR, Cavagna GA.** Energetics and mechanics of terrestrial locomotion. IV. Total mechanical energy changes as a function of speed and body size in birds and mammals. *J Exp Biol* 97: 57–66, 1982.
28. **Henry HT, Ellerby DJ, Marsh RL.** Performance of guinea fowl *Numida meleagris* during jumping requires storage and release of elastic energy. *J Exp Biol* 208: 3293–3302, 2005.
29. **Kram R.** Muscular force or work: what determines the metabolic energy cost of running? *Exerc Sport Sci Rev* 28: 138–143, 2000.
30. **Kram R, Taylor CR.** Energetics of running: a new perspective. *Nature* 346: 265–267, 1990.
31. **Kushmerick MJ, Larson RE, Davies RE.** The chemical energetics of muscle contraction. I. Activation heat, heat of shortening and ATP utilization for activation-relaxation processes. *Proc R Soc Lond B Biol Sci* 174: 293–313, 1969.
32. **Manabe N, Sato E, Izumi T, Ishibashi T.** Histoenzymatic characteristics and the size of skeletal muscle fibers in the guinea fowl Numida-Meleagris. *Jap J Ornith* 37: 1–16, 1988.
33. **Mansour JM, Audu ML.** The passive elastic moment at the knee and its influence on human gait. *J Biomech* 19: 369–373, 1986.
34. **Margaria R.** *Biomechanics and Energetics of Muscular Exercise*. Oxford, UK: Clarendon, 1976.
35. **Marsh RL, Ellerby DJ, Carr JA, Henry HT, Buchanan CI.** Partitioning the energetics of walking and running: swinging the limbs is expensive. *Science* 303: 80–83, 2004.
36. **Marsh RL, Ellerby DJ, Henry HT, Rubenson J.** The energetic costs of trunk and distal-limb loading during walking and running in guinea fowl *Numida meleagris*. I. Organismal metabolism and biomechanics. *J Exp Biol* 209: 2050–2063, 2006.
37. **Martin PE.** Mechanical and physiological responses to lower extremity loading during running. *Med Sci Sports Exerc* 17: 427–433, 1985.
38. **McDowell B, Cosgrove A, Baker R.** Estimating mechanical cost in subjects with myelomeningocele. *Gait Posture* 15: 25–31, 2002.
39. **Mills PM, Barrett RS.** Swing phase mechanics of healthy young and elderly men. *Hum Mov Sci* 20: 427–446, 2001.
40. **Mochon S, McMahon TA.** Ballistic walking. *J Biomech* 13: 49–57, 1980.
41. **Modica JR, Kram R.** Metabolic energy and muscular activity required for leg swing in running. *J Appl Physiol* 98: 2126–2131, 2005.
42. **Myers MJ, Steudel K.** Effect of limb mass and its distribution on the energetic cost of running. *J Exp Biol* 116: 363–373, 1985.
43. **Nelson FE, Gabaldon AM, Roberts TJ.** Force-velocity properties of two avian hindlimb muscles. *Comp Biochem Physiol A Mol Integr Physiol* 137: 711–721, 2004.
44. **Pontzer H.** A new model predicting locomotor cost from limb length via force production. *J Exp Biol* 208: 1513–1524, 2005.
45. **Purkiss SB, Robertson DG.** Methods for calculating internal mechanical work: comparison using elite runners. *Gait Posture* 18: 143–149, 2003.
46. **Riener R, Edrich T.** Identification of passive elastic joint moments in the lower extremities. *J Biomech* 32: 539–544, 1999.
47. **Roberts TJ, Chen MS, Taylor CR.** Energetics of bipedal running. II. Limb design and running mechanics. *J Exp Biol* 201: 2753–2762, 1998.
48. **Royer TD, Martin PE.** Manipulations of leg mass and moment of inertia: effects on energy cost of walking. *Med Sci Sports Exerc* 37: 649–656, 2005.
49. **Rubenson J, Henry HT, Dimoulas PM, Marsh RL.** The cost of running uphill: linking organismal and muscle energy use in guinea fowl (*Numida meleagris*). *J Exp Biol* 209: 2395–2408, 2006.
50. **Selles RW, Bussmann JB, Wagenaar RC, Stam HJ.** Effects of prosthetic mass and mass distribution on kinematics and energetics of prosthetic gait: a systematic review. *Arch Phys Med Rehabil* 80: 1593–1599, 1999.
51. **Selles RW, Korteland S, Van Soest AJ, Bussmann JB, Stam HJ.** Lower-leg inertial properties in transtibial amputees and control subjects and their influence on the swing phase during gait. *Arch Phys Med Rehabil* 84: 569–577, 2003.
52. **Silder A, Whittington B, Heiderscheit B, Thelen DG.** Identification of passive elastic joint moment-angle relationships in the lower extremity. *J Biomech* 40: 2628–2635, 2007.

53. **Simonson DC, DeFronzo RA.** Indirect calorimetry: methodological and interpretative problems. *Am J Physiol Endocrinol Metab* 258: E399–E412, 1990.
54. **Smith NP, Barclay CJ, Loiselle DS.** The efficiency of muscle contraction. *Prog Biophys Mol Biol* 88: 1–58, 2005.
55. **Steudel K.** The work and energetic cost of locomotion. I. The effects of limb mass distribution in quadrupeds. *J Exp Biol* 154: 273–285, 1990.
56. **Sutherland DH, Davids JR.** Common gait abnormalities of the knee in cerebral palsy. *Clin Orthop Relat Res* 288: 139–147, 1993.
57. **Taylor CR, Heglund NC, Maloiy GM.** Energetics and mechanics of terrestrial locomotion. I. Metabolic energy consumption as a function of speed and body size in birds and mammals. *J Exp Biol* 97: 1–21, 1982.
58. **Waters RL, Mulroy S.** The energy expenditure of normal and pathologic gait. *Gait Posture* 9: 207–231, 1999.
59. **Whittington B, Silder A, Heiderscheit B, Thelen DG.** The contribution of passive-elastic mechanisms to lower extremity joint kinetics during human walking. *Gait Posture* 27: 628–634, 2008.
60. **Willems PA, Cavagna GA, Heglund NC.** External, internal and total work in human locomotion. *J Exp Biol* 198: 379–393, 1995.
61. **Wilson AM, Watson JC, Lichtwark GA.** Biomechanics: a catapult action for rapid limb protraction. *Nature* 421: 35–36, 2003.
62. **Winter DA.** *Biomechanics and Motor Control of Human Movement*. New York: Wiley, 1990.
63. **Woledge RC, Curtin NA, Homsher E.** *Energetic Aspects of Muscle Contraction*. New York: Academic, 1985.
64. **Yoon YS, Mansour JM.** The passive elastic moment at the hip. *J Biomech* 15: 905–910, 1982.
65. **Zatsiorsky VM.** *Kinetics of Human Motion*. Champaign, IL: Human Kinetics, 2002.